https://doi.org/10.5194/egusphere-2026-6885
Preprint. Discussion started: 13 November 2026
© Author(s) 2026. CC BY 4.0 License.

Capillary Fringe Truncation Triggers a Transition from Drainage to Pressure Transmission in Riparian Aquifers: Laboratory Experiments

Haokun Mu[1,2], Xiuyu Liang[2,*], Dongchen Li[2], Jiayi Li[2], Chi-Yuen Wang[3]

[1]School of Environment, Harbin Institute of Technology, Harbin, Heilongjiang, China
[2]State Key Laboratory of Soil Pollution Control and Safety, School of Environmental Science and Engineering, Southern University of Science and Technology, Shenzhen, Guangdong, China
[3]Department of Earth and Planetary Science, University of California, Berkeley, CA, USA

*Corresponding author: Xiuyu Liang (liangxy@sustech.edu.cn)

https://doi.org/10.5194/egusphere-2026-6885
Preprint. Discussion started: 13 November 2026
© Author(s) 2026. CC BY 4.0 License.



Abstract

Understanding Earth's riparian ecosystems requires consideration of interactions between groundwater and the surfaces. Shallow riparian aquifers are commonly interpreted as drainage systems, where groundwater level changes reflect storage release and lateral exchange with rivers. Here we show that this interpretation may fail when the capillary fringe is truncated by the land surface. With a two-dimensional sand tank experiment, we show that, as truncation increased, recession changed from a delayed propagation to a synchronous head decline. Under the strongest truncation, cumulative drainage decreased by 94%, the recession-derived hydraulic diffusivity increased by more than one order of magnitude. Diagnostic models calibrated under the nontruncated condition could not reproduce truncated responses without reducing specific yield. These results reveal a shift from drainage-dominated to pressure-transmission-dominated behavior, where rapid head responses occur with limited water release, highlighting the need to consider capillary fringe truncation when interpreting hydraulic responses and lateral water exchange in riparian aquifers.

https://doi.org/10.5194/egusphere-2026-6885
Preprint. Discussion started: 13 November 2026
© Author(s) 2026. CC BY 4.0 License.

1 Introduction

Riparian aquifers function as a drainage interface between rivers and adjacent subsurface systems. They store groundwater and release it to streams as baseflow (Fig. 1a). Driven by the hydraulic gradients across riverbanks, it controls the river-groundwater exchange (Briggs & Hare, 2018; Hester & Fox, 2020) and shapes the subsurface flow paths, residence times, contaminant transport, and the hydrological conditions that make riparian zones hotspots of biogeochemical processes (Cey et al., 1998; McClain et al., 2003; Zarnetske et al., 2011; Cardenas, 2008; McCallum & Shanafield, 2016; Liang et al., 2018). Quantifying the groundwater dynamics in riparian aquifers is therefore essential for estimating baseflow, river-groundwater exchange fluxes, and the hydrological controls on river corridor biogeochemical function (Ledesma et al., 2025).

Riparian groundwater dynamics are commonly inferred from two types of observations: baseflow recession and groundwater level responses to river-stage fluctuations. Recession reflects the release of drainable storage, whereas river-stage responses reflect saturated zone pressure diffusion controlled by hydraulic diffusivity (Brutsaert & Nieber, 1977; Rupp & Selker, 2006; Nielsen, 1990; Liang & Zhang, 2012; Liang et al., 2017). River-groundwater exchanges are commonly estimated from measured or simulated hydraulic gradients using Darcy's law (Kalbus et al., 2006; Rosenberry & LaBaugh, 2008; Menció et al., 2014). These approaches linked the observed heads and discharge to storage release and advective exchange by assuming that groundwater dynamics are governed primarily by saturated zone drainage.

This assumption becomes uncertain in shallow riparian aquifers, where the water table can be close to the land surface for the capillary processes to influence both the storage release and the pressure propagation (Vogan et al., 2025). Previous studies have shown that unsaturated-zone

https://doi.org/10.5194/egusphere-2026-6885
Preprint. Discussion started: 13 November 2026
© Author(s) 2026. CC BY 4.0 License.

storage and delayed drainage can modify baseflow recession and river-groundwater interaction (Kong et al., 2015; Liang et al., 2017; Zhou et al., 2023; Wang et al., 2024; Wen et al., 2026; Li et al., 2026). A more specific control is the capillary fringe, where saturated water is held above the water table under negative pressure. This near-water-table storage can reduce drainable water associated with a given water-table change, making effective storage strongly state dependent (Gillham, 1984; Nachabe et al., 2004; Cartwright et al., 2009). This effect is particularly important in riparian aquifers, where shallow water tables and fine sediments can make capillary fringe thickness comparable to the unsaturated zone thickness.

When the capillary fringe reaches or exceeds the land surface, it is truncated by the upper boundary (gray region in Figure 1a). Previous studies have shown that capillary fringe truncation can produce abrupt water table changes, reduce dynamic effective porosity, and generate nearly zero lag water-table responses to periodic forcing (Cartwright et al., 2009; Zheng et al., 2022). Recent studies further suggest that truncation can affect lateral groundwater flow near rivers (Zheng et al., 2024). These studies showed that capillary fringe truncation alters water table dynamics, but its quantitative effects on groundwater recession and the river-groundwater exchange remain poorly understood.

To address this gap, we used controlled experiments to investigate how capillary fringe truncation alters hydraulic behavior relevant to shallow riparian aquifers. We conducted two-dimensional sand tank experiments under six truncation conditions, including drainage recession following boundary drawdown and fluctuating hydraulic head forcing at the boundary. Independent sand column drainage measurements the capillary fringe height. We combined observed hydraulic heads, drainage volumes, and diagnostic model comparisons to distinguish drainage associated with storage release from rapid pressure transmission under low-storage

https://doi.org/10.5194/egusphere-2026-6885
Preprint. Discussion started: 13 November 2026
© Author(s) 2026. CC BY 4.0 License.

conditions. These observations reveal that strong truncation reduces water release and lateral exchange but preserves rapid head propagation, indicating a transition from drainage to pressure transmission in riparian aquifers.

2 Materials and Methods

2.1 Experimental Setup and Truncation Conditions

Figure 1a illustrates the riparian setting represented in the experiments. Near a river, the water table may approach the land surface so that the depth to the water table, b, may become smaller than the fully developed capillary fringe height, B, causing the land surface to truncate the fringe. We simulate this condition in a two-dimensional sand tank experiment. The 79.2 cm long, 20 cm wide, and 40 cm high tank comprised a 70 cm porous medium domain and a 9.2 cm boundary reservoir (Figure 1b). Boundary head was controlled by a vertically movable overflow reservoir and monitored using a HOBO water-level data logger (U20-001-01-Ti, Onset Computer Corporation, USA). Hydraulic heads within the sand tank were measured at x=5, 15, 40, and 60 cm from the reservoir boundary using pressure transducers (CY201, Chengdu Keda Shengying Technology Co., Ltd., China), with all pressure transducers installed at z=10 cm above the tank base.

The tank was wet packed below the water surface with fully prewetted quartz sand with a representative grain size of 1 mm to minimize air entrapment. Independent sand column tests were conducted to characterize the hydraulic and capillary properties of the sand. A falling head test yielded a saturated hydraulic conductivity, K, of 0.121 cm/s. A stepwise drainage test following Cartwright et al. (2009) yielded a fully developed capillary fringe height, B, of 11 cm, defined as the maximum height sustained during water table decline. The same drainage test was

https://doi.org/10.5194/egusphere-2026-6885
Preprint. Discussion started: 13 November 2026
© Author(s) 2026. CC BY 4.0 License.

also used to quantify the state-dependent dynamic effective specific yield, S_y from the relation between cumulative drainage and water table decline. Details of the sand column tests and drainage analysis are provided in the Supporting Information (Text S1 and Figures S1-S2). Capillary fringe truncation is defined as (Cartwright et al., 2004; Zheng et al., 2022)

$$TF = \frac{b}{B} \tag{1}$$

The reference water table elevation was 22 cm above the tank base. This elevation was the initial head in the recession experiments and the upper boundary head in the periodic experiments. Six configurations were created by setting the sand surface at elevations of 37, 34, 31, 28, 25, and 22 cm (Figure 1c). The corresponding values of b were 15, 12, 9, 6, 3, and 0 cm, giving TF=15/11, 12/11, 9/11, 6/11, 3/11, and 0, respectively. At the reference water level, TF>1 indicates that the capillary fringe can fully develop below the sand surface, whereas TF<1 indicates truncation by the sand surface. The actual degree of truncation varied as the water table moved during recession and periodic forcing, while TF was used as a fixed index of each experimental configuration. This design systematically varied the position of the land surface relative to the capillary fringe while maintaining the same saturated zone properties and imposed boundary heads.

2.2 Recession and Periodic Boundary Forcing Experiments

Two sets of experiments were conducted at each truncation condition to characterize drainage recession and the response to boundary head fluctuations. For the recession experiments, the sand tank was first saturated by maintaining the river boundary head at 37 cm. The boundary head was then lowered to 22 cm, and the system was allowed to equilibrate for 1 h. After stabilization, the river boundary was lowered quickly to 11 cm and the outlet was opened to

https://doi.org/10.5194/egusphere-2026-6885
Preprint. Discussion started: 13 November 2026
© Author(s) 2026. CC BY 4.0 License.

initiate drainage toward the reservoir. The boundary head at the reservoir and hydraulic heads at the four observation locations of the sand tank were recorded at 1 s intervals. Outflow was collected continuously in a receiving container, and cumulative drainage from the sand tank was determined from the collected volume. The same boundary sequence was applied under all six truncation conditions. For the periodic boundary-forcing experiments, the system was first equilibrated at a boundary head of 22 cm. The boundary head was then varied sinusoidally between 13 and 22 cm with a period of 200 s. Nine cycles were imposed for each truncation condition, and the final two repeatable cycles were used for analysis.

2.3 Data Analysis and Diagnostic Modeling

For the recession experiments, drainage discharge was obtained from the time derivative of the cumulative drainage. After the initial transient response, the drainage recession was fitted using the following exponential relation (Brutsaert & Nieber, 1977)

$$Q = Q_0 \exp(-\beta t) \tag{2}$$

where Q is the drainage discharge [L^3/T]; Q_0 is the initial discharge [L^3/T]; and β is the recession coefficient [1/T]. For the linearized Boussinesq solution of groundwater recession in an unconfined aquifer, the recession coefficient β is related to hydraulic diffusivity by (Liang & Zhang, 2012)

$$\beta = \frac{\pi^2 D}{4L^2}, \qquad D = \frac{K\bar{h}}{S_y} \tag{3}$$

where D is the hydraulic diffusivity [L^2/T]; L is the distance between the reservoir boundary and the divide [L], which is 70 cm in the present sand tank; $\bar{h}$ is the average aquifer thickness [L]; and S_y is specific yield. Accordingly, hydraulic diffusivity can be estimated from the fitted recession coefficient as $D = 4L^2\beta/\pi^2$. The approximately linear portions of the semilogarithmic recession curves were used to estimate β. Because Equation (3) assumes recession is controlled

https://doi.org/10.5194/egusphere-2026-6885
Preprint. Discussion started: 13 November 2026
© Author(s) 2026. CC BY 4.0 License.

solely by saturated zone drainage, the estimated diffusivity is hereafter referred to as the apparent hydraulic diffusivity.

For the periodic experiments, the two repeatable cycles were analyzed. The amplitude and phase of the hydraulic head records at x=5, 15, 40, and 60 cm were obtained by least-squares fitting of a sinusoidal function with the imposed period of 200 s. Spatial attenuation was quantified by the amplitude ratio A_{60}/A_5, where A_5 and A_{60} are the amplitudes of groundwater heads at x=5 and 60 cm, respectively. The phase difference, $\Delta\phi$, between the hydraulic heads at x=5 and 60 cm were converted to a time lag as $\Delta t_{60-5} = \Delta\phi T/(2\pi)$, where T=200 s. The lateral hydraulic gradient between x=5 and 60 cm was calculated at each time step as $G(t) = [h_5(t) - h_{60}(t)]/55$, where $h_5(t)$ and $h_{60}(t)$ are the hydraulic heads at x=5 and 60 cm, respectively. The $G(t)$ time series during the final two repeatable cycles for all six TF conditions are shown in the Supporting Information (Figures S3). Because the imposed boundary head period was 200 s, each $G(t)$ series was fitted with a sinusoidal function of the same period, and its amplitude was defined as G_{amp}. Under strong truncation (TF = 3/11 and 0), the heads at x=5 and 60 cm became nearly synchronous, resulting in very small hydraulic gradients; consequently, small nonperiodic differences between the two head records became relatively more apparent and $G(t)$ deviated from an ideal sinusoidal form. The amplitude was therefore used to quantify the dominant periodic component of the lateral hydraulic gradient.

Two diagnostic models were used to interpret the periodic head responses: a one-dimensional nonlinear Boussinesq model representing saturated groundwater flow (hereafter referred to as the saturated model, Text S2.1) and a variably saturated Richards model with van Genuchten relations (hereafter referred to as the coupled model, Text S2.2). Both models were solved numerically using COMSOL Multiphysics. Two modeling scenarios were considered: the

https://doi.org/10.5194/egusphere-2026-6885
Preprint. Discussion started: 13 November 2026
© Author(s) 2026. CC BY 4.0 License.

parameter-transfer scenario and the TF-specific recalibration scenario. In the parameter-transfer scenario, both models were calibrated against the nontruncated case (TF = 15/11), and the calibrated parameters were then transferred unchanged to the other five truncation conditions. The saturated model parameters were unchanged across truncation conditions, whereas the coupled model differed only in vadose-zone thickness. This scenario tested whether the observed responses could be explained by the models without invoking truncation-dependent hydraulic properties. In the TF-specific recalibration scenario, both models were calibrated independently for each truncation condition by adjusting only the storage parameter S_y. In the saturated model, S_y represents the specific yield in the Boussinesq equation. In the coupled model, S_y represents the drainage porosity, defined as the difference between saturated and residual volumetric water contents. The drainage porosity was adjusted by varying the saturated water content while keeping the residual water content and the other van Genuchten parameters fixed. In both models, the saturated hydraulic conductivity was fixed at the independently measured value of 0.121 cm/s, because the same sand and saturated-zone configuration were used under all truncation conditions. Fixing hydraulic conductivity also avoided the strong parameter trade-off between conductivity and storage when fitting hydraulic head responses. The calibrated models were subsequently used to estimate lateral exchange across the reservoir boundary (Text 2.3; Figure S6). Detailed model formulations and calibration procedures are provided in Text S2 of the Supporting Information.

3 Results

3.1 Impacts of Capillary Fringe Truncation on Head Recession

Experimental observations showed that hydraulic head recession became progressively faster and more synchronous as TF decreased (Figure 2a). At TF = 15/11 and 12/11, the head response

https://doi.org/10.5194/egusphere-2026-6885
Preprint. Discussion started: 13 November 2026
© Author(s) 2026. CC BY 4.0 License.

was increasingly delayed with distance from the boundary, producing clear separation among the hydraulic-head curves during recession. A similar but weaker spatial lag remained at TF = 9/11. At TF = 6/11, the heads declined more rapidly and the differences among observation locations narrowed substantially. At TF = 3/11 and 0, the four hydraulic head curves nearly overlapped and approached the boundary head with little time lag (Figure 2b).

Because the saturated zone thickness and imposed boundary decline were unchanged among experiments, the reduced spatial lag can only be attributed to the increased capillary fringe truncation. Under weak to moderate truncation (TF $\geq$ 9/11), hydraulic heads declined progressively inland, consistent with a distributed drainage and storage release. Under strong truncation (TF $\leq$ 6/11), heads declined almost simultaneously across the sand tank, indicating that the boundary head change was transmitted mainly as a pressure response. Section 3.2 will show that this rapid head response was accompanied by sharply reduced water drainage.

3.2 Impacts of Capillary Fringe Truncation on Drainage Recession

Cumulative drainage decreased systematically with increasing capillary fringe truncation (Figure 3a). At 1,500 s, cumulative drainage decreased from 5.53 L at TF = 15/11 to 1.70 L at TF = 6/11, 0.61 L at TF = 3/11, and 0.33 L at TF = 0 (Figure 3b). The strongest truncation condition (TF=0) therefore reduced drainage by 94%, relative to TF = 15/11. This result is important when interpreted together with Figure 2: strong truncation produced faster and more synchronous head recession but released substantially less water from the sand tank.

Despite the large differences in cumulative drainage magnitude and duration, drainage recession remained approximately exponential under all truncation conditions (Figure 3c). The early stage showed some departures from the exponential form, whereas the subsequent

https://doi.org/10.5194/egusphere-2026-6885
Preprint. Discussion started: 13 November 2026
© Author(s) 2026. CC BY 4.0 License.

recession was well represented by Equation 2. The fitted β values remained 0.01 s^{-1} for TF = 15/11, 12/11, and 9/11. They increased to 0.02 s^{-1} at TF = 6/11 and to 0.15 and 0.11 s^{-1} at TF = 3/11 and 0, respectively (Figure 3c). Thus, capillary fringe truncation did not alter the overall exponential form of drainage recession, but it substantially increased the recession rate. The increase was not strictly monotonic, because β reached its maximum at TF = 3/11, but both strongly truncated conditions had values more than one order of magnitude larger than those under weak truncation. The apparent (estimated) hydraulic diffusivity remained near 20 cm^2/s for TF = 15/11, 12/11, and 9/11, increased to approximately 40 cm^2/s at TF = 6/11, and reached approximately 298 and 218 cm^2/s at TF = 3/11 and 0, respectively (Figure 3d). The apparent diffusivity at TF = 3/11 was 14.9 times that at TF = 15/11.

The apparent hydraulic diffusivity estimated from the drainage recession relation increased markedly with increasing capillary fringe truncation. Because hydraulic diffusivity depends on hydraulic conductivity, saturated zone thickness and specific yield, this change alone cannot be uniquely attributed to either parameter. However, the same sand and saturated-zone configuration were used in all experiments, and the independently measured hydraulic conductivity was therefore assumed to remain constant. Under this assumption, the increase in diffusivity corresponds to a decrease in specific yield. The inferred specific yield remained nearly constant under no or weak truncation (TF $\geq$ 9/11) but decreased rapidly once truncation became pronounced (TF $\leq$ 6/11). This trend is consistent with previous studies showing that capillary fringe truncation reduces specific yield (Gillham, 1984; Cartwright et al., 2005; Zheng et al., 2022). Independent column drainage measurements provide additional support for this interpretation: the dynamic specific yield was approximately 0.015 while the capillary fringe was

https://doi.org/10.5194/egusphere-2026-6885
Preprint. Discussion started: 13 November 2026
© Author(s) 2026. CC BY 4.0 License.

truncated and increased to approximately 0.32 after the capillary fringe became fully developed below the sand surface (Figure S2; Text S1.3).

3.3 Impacts of Capillary Fringe Truncation on Fluctuated Hydraulic Responses

Fluctuation experiments showed that hydraulic head responses changed markedly with capillary fringe truncation under periodic boundary-head forcing (Figure 4a). At TF = 15/11, 12/11, and 9/11, head fluctuation attenuated and lagged with distance from the boundary. Spatial attenuation and lag remained visible at TF = 6/11 but were substantially reduced. At TF = 3/11 and 0, the head curves at the four observation locations nearly overlapped, indicating an almost synchronous response across the sand tank.

The spatial amplitude ratio A_{60}/A_5 remained between 0.70 and 0.74 for TF = 15/11, 12/11, and 9/11, increased to 0.83 at TF = 6/11, and approached unity at TF = 3/11 and 0 (Figure 4b). Thus, strong truncation nearly eliminated the attenuation between x=5 and 60 cm. The phase lag $\Delta t_{60\text{-}5}$ declined in parallel (Figure 4c), remaining between 11.5 and 12.8 s for TF = 15/11, 12/11, and 9/11, decreasing to 7.5 s at TF = 6/11, and falling to 2.1 and 1.3 s at TF = 3/11 and 0, respectively. The largest changes in both amplitude attenuation and phase lag occurred between TF = 6/11 and 3/11, marking a transition to nearly synchronous head fluctuations under strong truncation. This response was consistent with the sharp reduction in recession propagation lag observed in the head recession experiment (Figure 2).

The fluctuated lateral hydraulic gradient showed an even stronger response to capillary fringe truncation (Figure 4d). The gradient amplitude G_{amp} remained nearly constant between 0.028 and 0.029 for TF = 15/11, 12/11, and 9/11, but decreased to 0.019 at TF = 6/11 and fell sharply to 0.005 and 0.003 at TF = 3/11 and 0, respectively. Relative to TF = 15/11, the gradient amplitude

https://doi.org/10.5194/egusphere-2026-6885
Preprint. Discussion started: 13 November 2026
© Author(s) 2026. CC BY 4.0 License.

was reduced by approximately 83% at TF = 3/11 and 90% at TF = 0. Thus, the nearly synchronous groundwater fluctuations under strong truncation were accompanied by substantially smaller lateral gradients.

The fluctuation experiments reveal a coordinated change in hydraulic response as truncation increased: spatial amplitude attenuation and phase lag progressively disappeared, while the lateral hydraulic gradient decreased sharply. All three metrics changed little from TF = 15/11 to 9/11, showed an intermediate response at TF = 6/11, and changed most strongly between TF = 6/11 and 3/11. This pattern independently confirms the transition observed during drainage recession in Figure 2. The implications of the reduced hydraulic gradients for boundary exchange and model performance are evaluated next.

3.4 Model Representation of Hydraulic Heads and Lateral Exchange

The performance of the two diagnostic models is illustrated at x=5 and 40 cm in Figures 5a and 5b. Complete model-observation comparisons are provided in Figures S4 and S5, and the model parameters are summarized in Tables S1 and S2. In the parameter-constant scenario, the prediction from the saturated model become increasingly deviated from observations as truncation increased (Figure 5a). On the other hand, the coupled model captured much of the observed change by accounting for the reduced vadose-zone thickness, but substantial discrepancies remained under strong truncation (TF<6/11). The model-observation mismatch, quantified by the root mean square error (RMSE), increased from approximately 0.81 cm at TF = 15/11 to 1.96 cm at TF = 0 for the saturated model, and from 0.84 to 1.42 cm for the coupled model (Figure 5c). These results show that the observation responses under truncated conditions could not be reproduced by both models using the parameter values obtained from the

https://doi.org/10.5194/egusphere-2026-6885
Preprint. Discussion started: 13 November 2026
© Author(s) 2026. CC BY 4.0 License.

nontruncated case (TF=15/11), even when the coupled model accounted for the reduced vadose-zone thickness.

In the TF-specific recalibration scenario, both models reproduced the observed head responses more closely, particularly under strong truncation (Figure 5b), with substantially lower RMSE values than in the parameter-constant scenario (Figure 5c). This improvement required a pronounced reduction in the fitted storage parameter as truncation increased (Figure 5d). For comparison, this parameter is denoted Sy in both models: it represents conventional specific yield in the saturated model and the difference between saturated and residual water contents in the coupled model. Sy decreased from approximately 0.015 at TF = 15/11 to 0.0004 at TF = 0 in the saturated model, and from approximately 0.024 to 0.0002 in the coupled model. Because K and the saturated zone thickness were unchanged among experiments, the systematic decrease in the fitted Sy indicates that the truncation-dependent response was represented primarily through a reduction in the effective drainage storage.

The two modeling scenarios also produced different predictions of lateral exchange across the head boundary. For each simulation, the amplitude of the simulated exchange time series was extracted at the imposed period of 200 s and normalized by the corresponding amplitude at TF = 15/11 (Figure 5e). The complete exchange time series are provided in Figure S6. In the parameter-constant scenario, the saturated model predicted only minor variations in exchange amplitude, reflecting slight differences in the imposed boundary-head forcing among experiments, whereas the coupled model predicted a reduction in exchange amplitude to approximately 0.36 at TF = 0 as the vadose-zone thickness decreased. Compared with the parameter-constant scenario, TF-specific recalibration resulted in a much clearer decrease in normalized exchange amplitude with increasing truncation for both models. At TF = 0, the

https://doi.org/10.5194/egusphere-2026-6885
Preprint. Discussion started: 13 November 2026
© Author(s) 2026. CC BY 4.0 License.

exchange amplitude decreased to approximately 0.13 for the saturated model and 0.0045 for the coupled model. Thus, using models calibrated under the nontruncated condition to predict strongly truncated conditions substantially overestimate exchange flux at the reservoir boundary. This overestimation was greatest for the saturated model but was also evident for the coupled model.

4 Discussion

Capillary fringe truncation changed the relationship between hydraulic response and water release. Strong truncation produced rapid, nearly synchronous heads but substantially less drainage and smaller lateral hydraulic gradients, supporting a shift toward pressure transmission dominated behavior. Earlier studies established rapid water-table responses and reduced dynamic effective porosity under truncation (Gillham, 1984; Cartwright et al., 2009; Zheng et al., 2022, 2023). Our experiments extend these findings by linking head propagation, drainage recession, and spatial hydraulic gradients within the same system. The broader implication is that the drainage behavior of shallow riparian aquifers can depend strongly on capillary configuration.

The recession results demonstrate why this matters for hydraulic parameter estimation. Recession remained approximately exponential, although its rate increased markedly under strong truncation. Thus, an exponential recession curve does not necessarily indicate drainage governed by constant aquifer properties. Under the saturated recession relation, fixing hydraulic conductivity and the reference saturated thickness translates the increased apparent diffusivity into a smaller apparent specific yield. Recession-derived storage parameters should therefore be interpreted in relation to water-table depth and capillary configuration. Applying a specific yield obtained under nontruncated conditions to a strongly truncated state could overestimate the water

https://doi.org/10.5194/egusphere-2026-6885
Preprint. Discussion started: 13 November 2026
© Author(s) 2026. CC BY 4.0 License.



released for a given head decline. The independent column experiments support this interpretation by showing a similar reduction in specific yield under truncation, although the estimated values differ because of different experimental conditions and timescales.

The modeling results reveal a related limitation in prediction. Parameters calibrated under the nontruncated condition did not reproduce the strongly truncated responses, even when the coupled model accounted for the reduced vadose-zone thickness. Recalibration improved the simulations by reducing effective storage but required observations from each truncation condition. The fitted parameters therefore describe condition-dependent storage rather than a single transferable material property. Both models also predicted larger exchange amplitudes with the transferred parameters than after recalibration. This suggests that models calibrated under nontruncated conditions may overestimate exchange when applied to strongly truncated systems. Because exchange flux was not measured directly, the potential overestimation cannot be confirmed by the experiments. Future models should account for the effects of capillary fringe truncation on effective storage, allowing different truncation conditions to be simulated without recalibrating Sy for each state.

For river-groundwater studies, these findings emphasize the need to distinguish hydraulic communication from advective exchange. Water-level fluctuations indicate a hydraulic response, but do not by themselves quantify water renewal or the delivery of dissolved constituents. This distinction matters when assessing riparian biogeochemical function: reduced exchange may limit reactant supply even where hydraulic responses remain pronounced. The present experiments establish the hydraulic basis for this possibility, but tracer and reactive-transport measurements are needed to determine its consequences.

https://doi.org/10.5194/egusphere-2026-6885
Preprint. Discussion started: 13 November 2026
© Author(s) 2026. CC BY 4.0 License.

Several limitations should qualify these conclusions. The experiments used homogeneous sand, a simplified two-dimensional geometry and one capillary fringe height. Truncation was also imposed by changing the sand-surface elevation, so vadose-zone thickness and capillary fringe truncation varied together; consequently, the transition between TF = 6/11 and 3/11 should not be interpreted as a universal threshold. Lateral exchange was not measured directly but inferred from model simulations. The present study was based on controlled laboratory experiments, future work should extend these findings to field-scale riparian aquifers to evaluate how capillary-fringe truncation influences recession, river-stage responses, and river-groundwater connectivity under natural conditions.

5 Conclusions

We used two-dimensional sand tank experiments and diagnostic flow modeling to investigate the effect of capillary fringe truncation on the hydraulic behavior of shallow riparian aquifers. The recession experiments showed that strong truncation produced faster and nearly synchronous head decline while reducing cumulative drainage by 94%. Drainage recession remained approximately exponential, but the recession-derived hydraulic diffusivity increased with truncation and was more than one order of magnitude higher under strong truncation than under the nontruncated condition. The fluctuation experiments showed that, under strong truncation, amplitude attenuation and phase lag nearly disappeared, while the lateral hydraulic-gradient amplitude decreased by 90%. Both experiments indicated a pronounced reduction in drainage storage with increasing truncation. Existing models could reproduce the observations only through truncation-dependent adjustment of specific yield, highlighting the need to explicitly represent capillary fringe truncation. Otherwise, models may overestimate river-groundwater exchange under truncated conditions.

https://doi.org/10.5194/egusphere-2026-6885
Preprint. Discussion started: 13 November 2026
© Author(s) 2026. CC BY 4.0 License.

Data availability

The experimental data in this study could be found in additional dataset (Mu et al., 2026).

Author contributions

Conceptualization: XL, HM. Methodology: XL, HM, DL, JL. Software: HM, JL. Validation: XL, HM. Investigation: XL, HM, CYW. Data curation: HM, DL, JL. Writing - Original Draft: HM, XL. Writing - Review and Editing: HM, XL, CYW. Supervision: XL. Funding acquisition: XL.

Competing interests

The contact author has declared that none of the authors has any competing interests.

Acknowledgments

This study was partially supported by the National Natural Science Foundation of China (Grant No. 42372289), the Fundamental and Interdisciplinary Disciplines Breakthrough Plan of the Ministry of Education of China (JYB2025XDXM 909), and the High-level University Special Fund (G03034K010).

References

Abdul, A. S., & Gillham, R. W. (1984). Laboratory Studies of the Effects of the Capillary Fringe on Streamflow Generation. *Water Resources Research*, *20*(6), 691-698. https://doi.org/10.1029/WR020i006p00691

Abdul, A. S., & Gillham, R. W. (1989). Field studies of the effects of the capillary fringe on streamflow generation. *Journal of Hydrology (Amsterdam)*, *112*(1), 1-18. https://doi.org/10.1016/0022-1694(89)90177-7

Baird, A. J., & Low, R. G. (2022). The water table: Its conceptual basis, its measurement and its usefulness as a hydrological variable. *Hydrological Processes*, *36*(6). https://doi.org/10.1002/hyp.14622

Bear, J. (1972). *Dynamics of Fluids in Porous Media* (1st ed.). Dover Publications.

Blowes, D. W., & Gillham, R. W. (1988). The generation and quality of streamflow on inactive uranium tailings near Elliot Lake, Ontario. *Journal of Hydrology (Amsterdam)*, *97*(1), 1-22. https://doi.org/10.1016/0022-1694(88)90062-5

https://doi.org/10.5194/egusphere-2026-6885
Preprint. Discussion started: 13 November 2026
© Author(s) 2026. CC BY 4.0 License.



Briggs, M. A., & Hare, D. K. (2018). Explicit consideration of preferential groundwater discharges as surface water ecosystem control points. *Hydrological Processes*, *32*(15), 2435-2440. https://doi.org/10.1002/hyp.13178

Brutsaert, W., & Nieber, J. L. (1977). Regionalized drought flow hydrographs from a mature glaciated plateau. *Water Resources Research*, *13*(3), 637-643. https://doi.org/10.1029/WR013i003p00637

Cartwright, N., Nielsen, P., & Dunn, S. (2003). Water table waves in an unconfined aquifer: Experiments and modeling. *Water Resources Research*, *39*(12). https://doi.org/10.1029/2003WR002185

Cartwright, N., Nielsen, P., & Li, L. (2004). Experimental observations of watertable waves in an unconfined aquifer with a sloping boundary. *Advances in Water Resources*, *27*(10), 991-1004. https://doi.org/10.1016/j.advwatres.2004.08.006

Cartwright, N., Nielsen, P., & Perrochet, P. (2009). Behavior of a shallow water table under periodic flow conditions. *Water Resources Research*, *45*(3). https://doi.org/10.1029/2008WR007306

Cey, E. E., Rudolph, D. L., Parkin, G. W., & Aravena, R. (1998). Quantifying groundwater discharge to a small perennial stream in southern Ontario, Canada. *Journal of Hydrology (Amsterdam)*, *210*(1), 21-37. https://doi.org/10.1016/S0022-1694(98)00172-3

Freeze, R. A., & Cherry, J. A. (1979). *Groundwater*. Englewood Cliffs, NJ: Prentice-Hall.

Gillham, R. W. (1984). The capillary fringe and its effect on water table response. *Journal of Hydrology (Amsterdam)*, *67*(1), 307-324. https://doi.org/10.1016/0022-1694(84)90248-8

Hall, F. R. (1968). Base-Flow Recessions-A Review. *Water Resources Research*, *4*(5), 973-983. https://doi.org/10.1029/WR004i005p00973

Hester, E. T., & Fox, G. A. (2020). Preferential Flow in Riparian Groundwater: Gateways for Watershed Solute Transport and Implications for Water Quality Management. *Water Resources Research*, *56*(12). https://doi.org/10.1029/2020WR028186

Kong, J., Xin, P., Hua, G.-F., Luo, Z.-Y., Shen, C.-J., Chen, D., & Li, L. (2015). Effects of vadose zone on groundwater table fluctuations in unconfined aquifers. *Journal of Hydrology (Amsterdam)*, *528*, 397-407. https://doi.org/10.1016/j.jhydrol.2015.06.045

Kroszynski, U. I., & Dagan, G. (1975). Well pumping in unconfined aquifers: The influence of the unsaturated zone. *Water Resources Research*, *11*(3), 479-490. https://doi.org/10.1029/WR011i003p00479

Ledesma, J. L. J., Musolff, A., Sponseller, R. A., Lupon, A., Peñarroya, X., Jativa, C., & Bernal, S. (2025). The Riparian Zone Controls Headwater Hydrology and Biogeochemistry, Doesn't It? Reassessing Linkages Across European Ecoregions. *Global Biogeochemical Cycles*, *39*(2). https://doi.org/10.1029/2024GB008250

Li, P., Liang, X., Zeng, L., Wang, G., Zhang, J., & Ma, E. (2026). Effects of the unsaturated zone on leaky aquifer groundwater dynamics induced by tidal rivers. *Journal of Hydrology (Amsterdam)*, *664*, Article 134607. https://doi.org/10.1016/j.jhydrol.2025.134607

https://doi.org/10.5194/egusphere-2026-6885
Preprint. Discussion started: 13 November 2026
© Author(s) 2026. CC BY 4.0 License.



Liang, X., & Zhang, Y.-K. (2012). Analytical Solution for Drainage and Recession from an Unconfined Aquifer. *Ground Water*, *50*(5), 793-798. https://doi.org/10.1111/j.1745-6584.2011.00867.x

Liang, X., Zhan, H., Zhang, Y., & Schilling, K. (2017). Base flow recession from unsaturated-saturated porous media considering lateral unsaturated discharge and aquifer compressibility. *Water Resources Research*, *53*(9), 7832-7852. https://doi.org/10.1002/2017WR020938

McClain, M. E., Boyer, E. W., Dent, C. L., Gergel, S. E., Grimm, N. B., Groffman, P. M., Hart, S. C., Harvey, J. W., Johnston, C. A., Mayorga, E., McDowell, W. H., & Pinay, G. (2003). Biogeochemical Hot Spots and Hot Moments at the Interface of Terrestrial and Aquatic Ecosystems. *Ecosystems (New York)*, *6*(4), 301-312. https://doi.org/10.1007/s10021-003-0161-9

Mu, H., Liang, X., Li, D., Li, J., & Wang, C.-Y. (2026). Experimental data on capillary fringe truncation and hydraulic responses in a two-dimensional sand tank. Science Data Bank. https://www.scidb.cn/en/s/7b6zQn

Nachabe, M., Masek, C., & Obeysekera, J. (2004). Observations and modeling of profile soil water storage above a shallow water table. *Soil Science Society of America Journal*, *68*(3), 719-724. https://doi.org/10.2136/sssaj2004.7190

Neilsen, G. H., Culley, J. L., & Cameron, D. R. (1980). Nonpoint N Runoff from Agricultural Watersheds into the Great Lakes. *Journal of Great Lakes Research*, *6*(3), 195-202. https://doi.org/10.1016/S0380-1330(80)72100-7

Nielsen, P., & Perrochet, P. (2000). Watertable dynamics under capillary fringes: experiments and modelling. *Advances in Water Resources*, *23*(5), 503-515. https://doi.org/10.1016/S0309-1708(99)00038-X

Philip, J. R. (1969). Hydrostatics and hydrodynamics in swelling soils. *Water Resources Research*, *5*(5), 1070-1077. https://doi.org/10.1029/WR005i005p01070

Rupp, D. E., & Selker, J. S. (2006). On the use of the Boussinesq equation for interpreting recession hydrographs from sloping aquifers. *Water Resources Research*, *42*(12). https://doi.org/10.1029/2006WR005080

Shoushtari, S. M. H. J., Cartwright, N., Nielsen, P., & Perrochet, P. (2016). The effects of oscillation period on groundwater wave dispersion in a sandy unconfined aquifer: Sand flume experiments and modelling. *Journal of Hydrology (Amsterdam)*, *533*, 412-420. https://doi.org/10.1016/j.jhydrol.2015.12.032

Szilagyi, J., Parlange, M. B., & Albertson, J. D. (1998). Recession flow analysis for aquifer parameter determination. *Water Resources Research*, *34*(7), 1851-1857. https://doi.org/10.1029/98WR01009

Vogan, J., Shikaze, S., & Doerken, K. (2025). R.W. Gillham and the Role of Capillary Fringe Processes in Shallow Aquifer Behavior. *Ground Water*, *63*(2), 291-294. https://doi.org/10.1111/gwat.13468

https://doi.org/10.5194/egusphere-2026-6885
Preprint. Discussion started: 13 November 2026
© Author(s) 2026. CC BY 4.0 License.



Wang, C.-Y., Zhu, A.-Y., Liao, X., Manga, M., & Wang, L.-P. (2019). Capillary effects on groundwater response to Earth tides. *Water Resources Research, 55*(8), 6886-6895. https://doi.org/10.1029/2019WR025166

Wang, C.-Y., Wang, L.-P., Manga, M., & Liang, X. (2024). Groundwater-Surface Interaction Amplified Post-Seismic Streamflow Fluctuation. *Communications Earth & Environment, 5*(1), Article 612. https://doi.org/10.1038/s43247-024-01735-7

Wang, G., Liang, X., Li, J., Wang, J., & Wang, C. (2024). Impact of Depth-Dependent Heterogeneity in Aquifers on the Response of Unsaturated-Saturated Flow to Earth Tides. *Water Resources Research*, *60*(6), Article e2023WR036310. https://doi.org/10.1029/2023WR036310

Wen, C., Liang, X., Zhan, H., Mu, H., & Zhou, Y. (2026). Analytical solutions for coupled unsaturated-saturated flow model in riparian zones: applicability and limitations. *Journal of Hydrology (Amsterdam)*, *668*, Article 135035. https://doi.org/10.1016/j.jhydrol.2026.135035

Zheng, Y., Yang, M., & Liu, H. (2022). The Effects of Truncating the Capillary Fringe on Water-Table Dynamics During Periodic Forcing. *Water Resources Research*, *58*(1), Article e2021WR031112. https://doi.org/10.1029/2021WR031112

Zheng, Y., Yang, M., & Liu, H. (2024). Coastal groundwater dynamics with a focus on wave effects. *Earth-Science Reviews*, *256*, Article 104869. https://doi.org/10.1016/j.earscirev.2024.104869

Zhou, Y. Q., Liang, X. Y., Ma, E. Z., Chen, K. W., Schilling, K. E., Zheng, T. Y., Zheng, Y. H., Zhang, Y.-K., & Zheng, C. M. (2024). Spectral analysis of hydrological signals to estimate watershed properties considering impacts of unsaturated zone. *Water Resources Research, 60*(11), e2023WR036680. DOI: 10.1029/2023WR036680.

Zhou, Y. Q., Liang, X. Y., Ma, E. Z., Chen, K. W., Zhang, J. W., & Zhang, Y.-K. (2023). Effect of unsaturated flow on groundwater-river interactions induced by flood event in riparian zone. *Journal of Hydrology, 620*, 129405. https://doi.org/10.1016/j.jhydrol.2023.129405

https://doi.org/10.5194/egusphere-2026-6885
Preprint. Discussion started: 13 November 2026
© Author(s) 2026. CC BY 4.0 License.

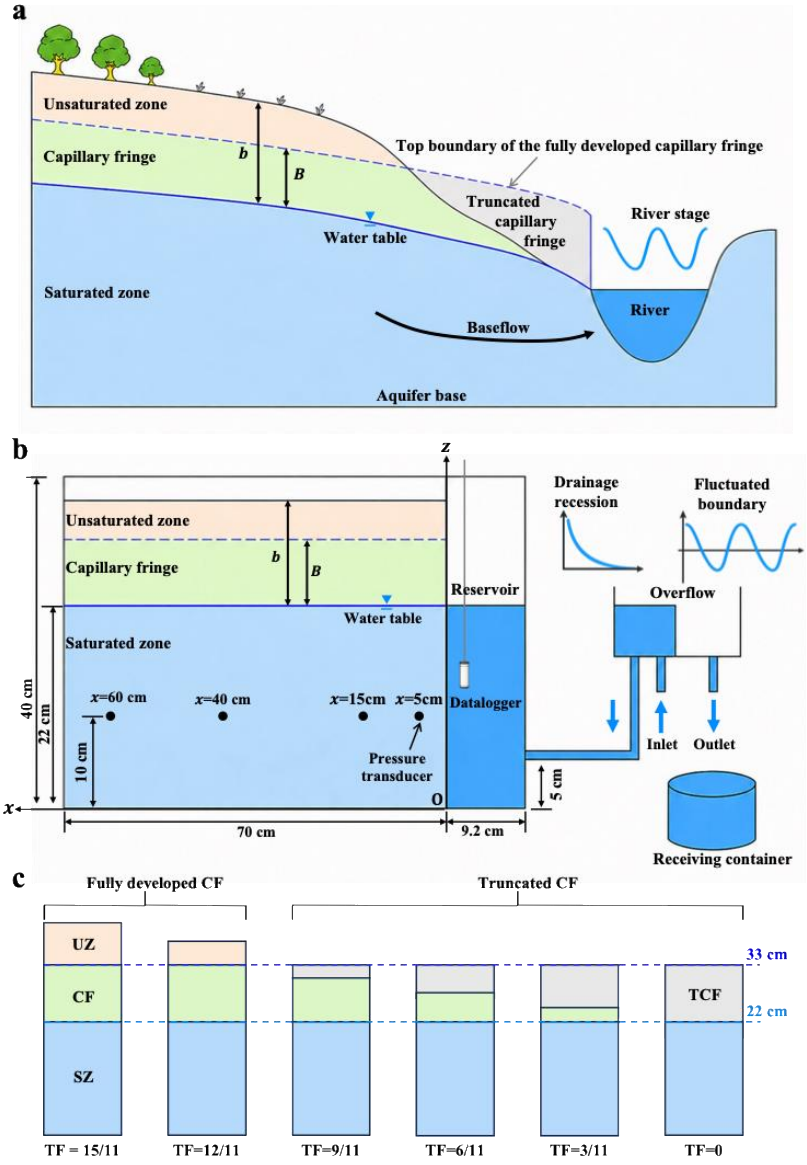


Figure 1. (a) The conceptual riparian model where, the capillary fringe, with a maximum height *B*, is truncated by the ground surface (define *b*) near the river (gray area). (b) Experimental design of a two-dimensional sand tank. Hydraulic head is measured at distances x=5, 15, 40, and 60 cm from the reservoir boundary. (c) Six truncation configurations at a reference water-table elevation of 22 cm. The dashed line marks the top of the 11 cm capillary fringe; colors denote the unsaturated zone (UZ), capillary fringe (CF), saturated zone (SZ), and truncated capillary fringe (TCF).

https://doi.org/10.5194/egusphere-2026-6885
Preprint. Discussion started: 13 November 2026
© Author(s) 2026. CC BY 4.0 License.

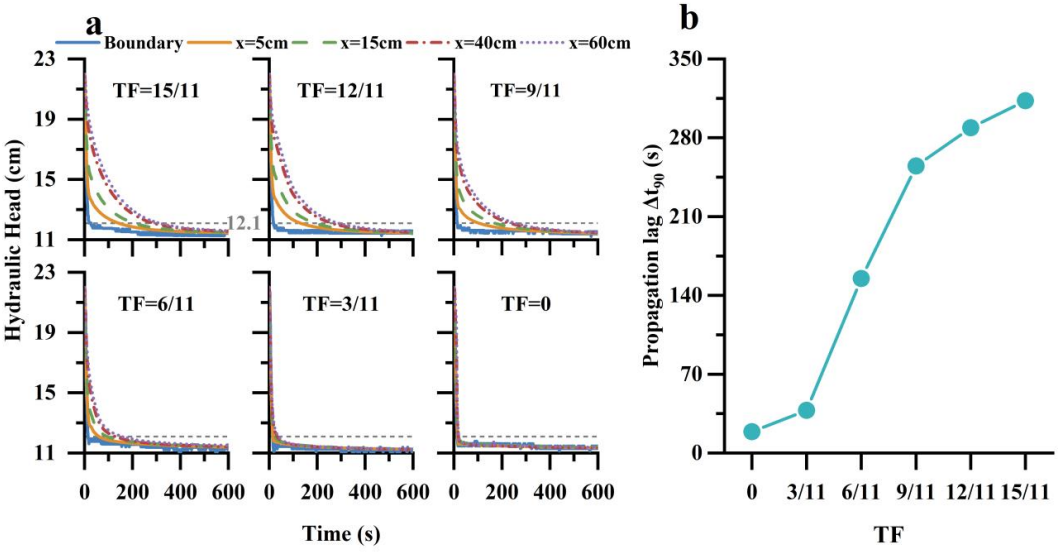


Figure 2. Hydraulic head recession at different capillary fringe truncation. (a) Boundary head and hydraulic heads at x=5, 15, 40, and 60 cm under six truncation factors. (b) Propagation lag, Δt_{90} , defined as the time difference between x=60 and x=5 cm for the head to decline to 12.1 cm, corresponding to 90% of the total drawdown.

https://doi.org/10.5194/egusphere-2026-6885
Preprint. Discussion started: 13 November 2026
© Author(s) 2026. CC BY 4.0 License.

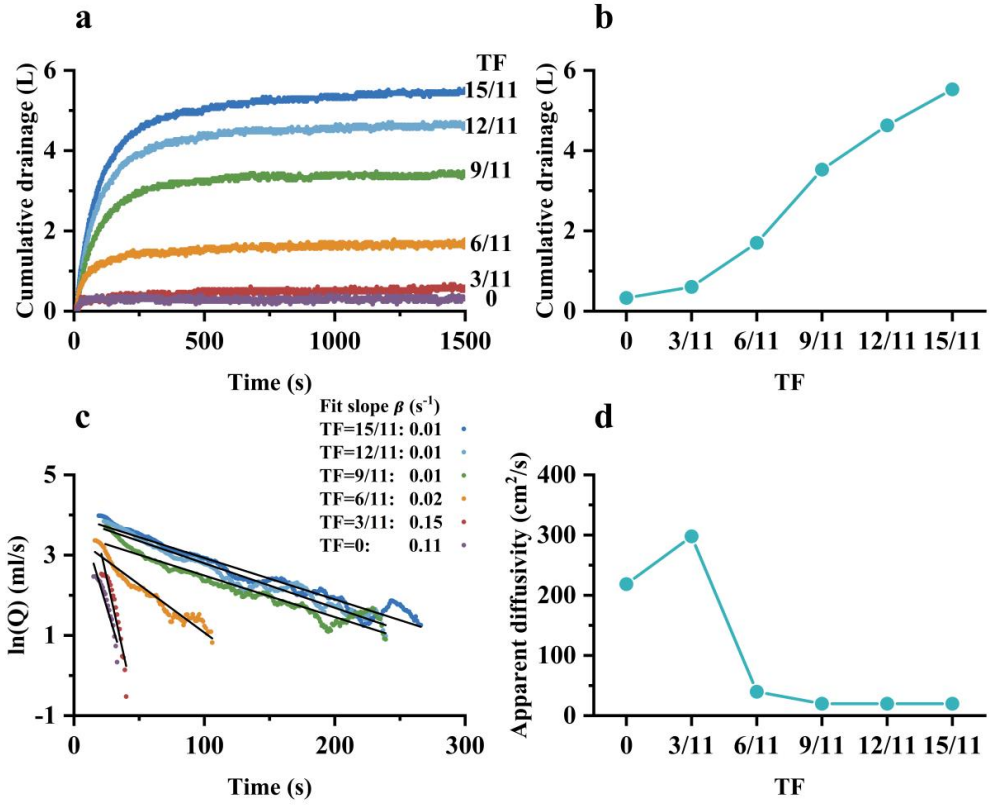


Figure 3. (a) Cumulative drainage under six TF conditions. (b) Cumulative drainage measured at 1,500 s. (c) Semilogarithmic drainage recession curves. Colored data show the observed discharge response, and dark lines show exponential regressions used to determine the recession coefficient β from $Q = Q_0 \exp(-\beta t)$. (d) Apparent hydraulic diffusivity estimated from the classical saturated recession relation, $D = 4\beta L^2/\pi^2$, where L=70 cm.

https://doi.org/10.5194/egusphere-2026-6885
Preprint. Discussion started: 13 November 2026
© Author(s) 2026. CC BY 4.0 License.

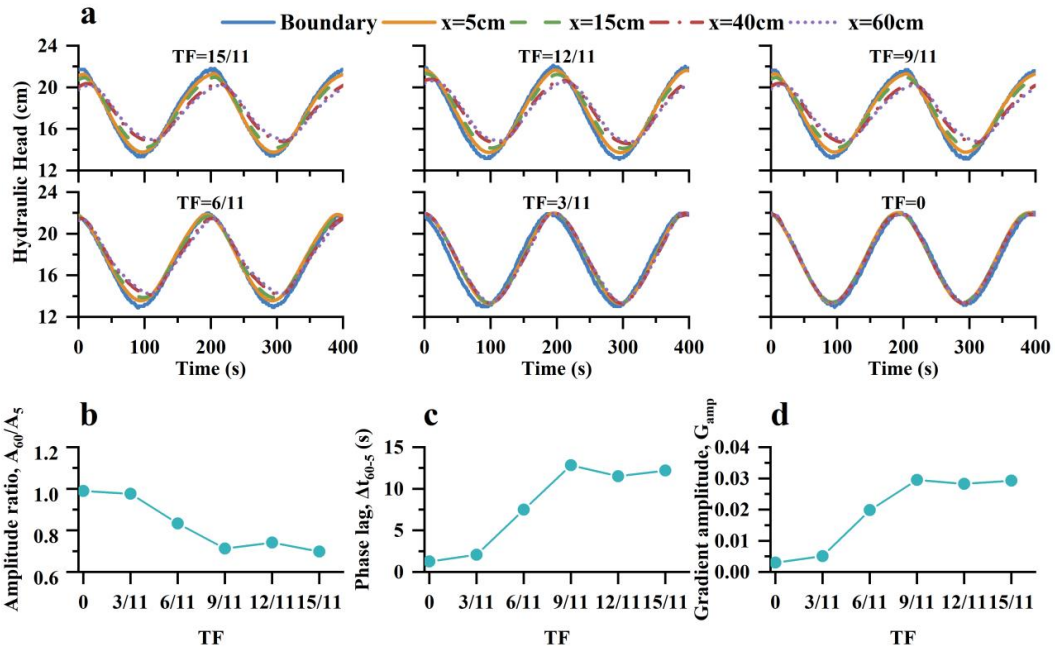


Figure 4. (a) Observed heads during the final stable cycle at x=5, 15, 40, and 60 cm under six TF conditions. (b) Spatial amplitude ratio, A_{60}/A_5, where A_5 and A_{60} are the amplitudes of heads at x=5 and 60 cm, respectively. (c) Phase lag $\Delta t_{60\text{-}5}$ between heads at x=5 and 60 cm. (d) Amplitude G_{amp} of the periodic lateral hydraulic-gradient time series between x=5 and 60 cm over the final two repeatable cycles (Figure S3).

https://doi.org/10.5194/egusphere-2026-6885
Preprint. Discussion started: 13 November 2026
© Author(s) 2026. CC BY 4.0 License.

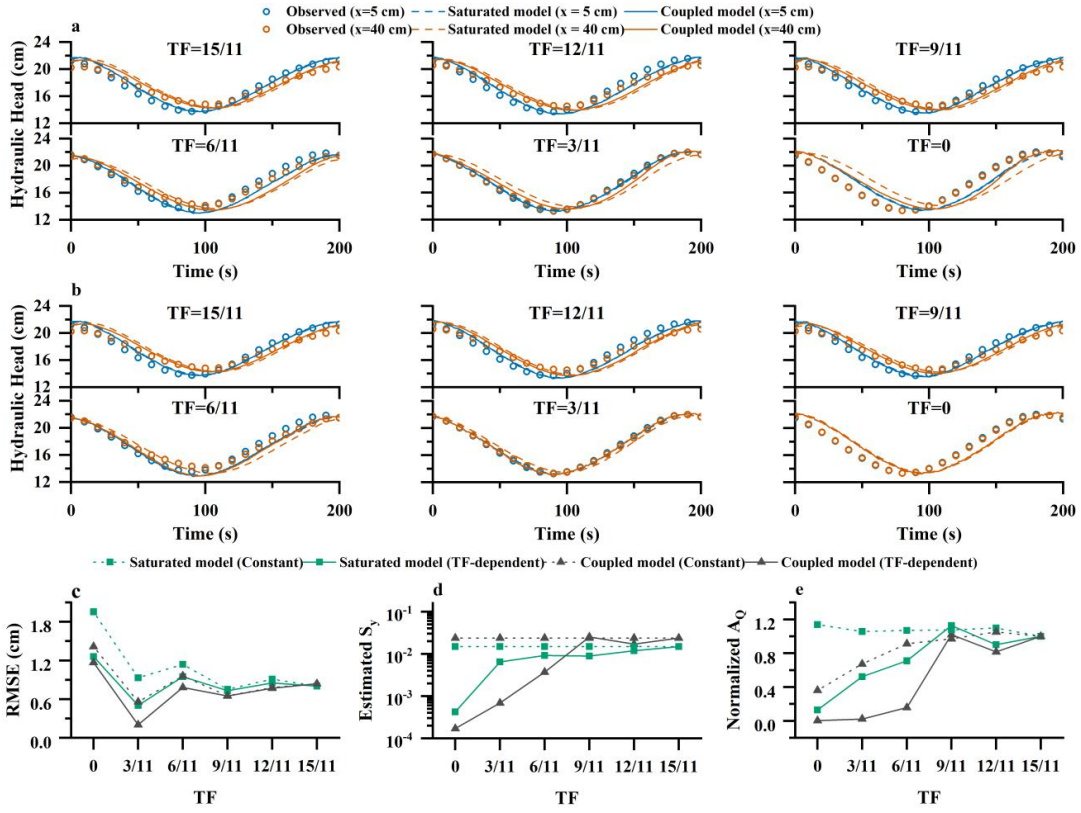


Figure 5. (a) Observed and simulated hydraulic heads at x=5 and 40 cm for the parameter-constant scenario. (b) Same as (a), but for the TF-specific recalibration scenario. (c) RMSE for the two models and modeling scenarios. (d) Estimated Specific yield Sy for the two scenarios. (e) Lateral exchange across the head boundary, normalized by the corresponding value at TF = 15/11. Open circles denote observations; dashed and solid lines in (a) and (b) denote the saturated and coupled models, respectively.